Radiocarbon Evidence for a Possible Abyssal Front Near 3.1 km in the Glacial Equatorial Pacific Ocean

L. D. Keigwin[a]*

S. J. Lehman[b]

[a]Woods Hole Oceanographic Institution
260 Woods Hole Rd.
Woods Hole, MA 02543

[b]University of Colorado
INSTAAR Campus Box 450
Boulder, CO 80309

*corresponding author
telephone 508 289 2784
email: lkeigwin@whoi.edu

ABSTRACT

We investigate the radiocarbon ventilation age in deep equatorial Pacific sediment cores using the difference in conventional ^{14}C age between coexisting benthic and planktonic foraminifera, and integrate those results with similar data from around the North Pacific Ocean in a reconstruction for the last glaciation (15 to 25 conventional ^{14}C ka). Most new data from both the Equatorial Pacific and the Emperor Seamounts in the northwestern Pacific come from maxima in abundance of benthic taxa because this strategy reduces the effect of bioturbation. Although there remains considerable scatter in the ventilation age estimates, on average, ventilation ages in the Equatorial Pacific were significantly greater below 3.2 km (~3080 ±1125 yrs, n=15) than in the depth interval 1.9 to 3.0 km (~1610 ± 250 yrs, n=12). When compared to the average modern seawater $\Delta^{14}C$ profile for the North Pacific, the Equatorial Pacific glacial data suggest an abyssal front located somewhere between 3.0 and 3.2 km modern water depth. Above that depth, the data may indicate slightly better ventilation than today, and below that depth, glacial Equatorial Pacific data appear to be as old as last glacial maximum (LGM) deep water ages reported for the deep southern Atlantic. This suggests that a glacial reservoir of aged waters extended throughout the circumpolar Southern Ocean

and into the Equatorial Pacific. Renewed ventilation of such a large volume of aged (and, by corollary, carbon-rich) water would help to account for the rise in atmospheric pCO_2 and the fall in $\Delta^{14}C$ as the glaciation drew to a close.

Key Words: radiocarbon; foraminifera; ocean ventilation; Pacific Ocean

1.0 INTRODUCTION

The ocean is the largest reservoir of readily exchangeable carbon on Earth. With ~39,000 gigatonnes of carbon (GTC = 10^{15} g C) in the ocean, and ~580 GTC in the recent pre-industrial atmosphere, it is clear that small changes in oceanic carbon storage could cause large changes in the atmospheric CO_2 inventory. For this reason, beginning ~25 years ago with ice core observations that the glacial atmosphere had lower CO_2 levels than today (Barnola et al., 1987; Petit et al., 1999), climatologists have looked to the ocean for evidence that its carbon storage was different in the past. Although the surface ocean readily exchanges with the atmosphere if it is not ice covered, the deep ocean exchanges with the atmosphere only at high latitude locations in the North Atlantic and Southern Oceans. Multiple lines of geochemical evidence indicate this exchange was interrupted during cold episodes of the last glacial cycle, either through the stabilizing effects of low salinity at sites of deep-water formation, sea ice cover at those sites, or both (Boyle, 1988; Duplessy et al., 1988; Sigman et al., 2010).

Unlike other proxies of deep ocean ventilation, radiocarbon comes with a timescale. Deep ocean ^{14}C content is set by the atmospheric ^{14}C activity and the extent of surface ocean equilibration with the atmosphere in the formation region, and decreases quantitatively due to radioactive decay in the ocean interior and may be further influenced by mixing. Available data from solitary corals and foraminifera indicate greater ventilation ages during the last ice age in the North Atlantic (Robinson et al. 2005), the South Atlantic (Skinner et al., 2010), and in the southwest Pacific (Skinner et al. 2015), but the most recent compilations from the Equatorial and North Pacific have failed to identify deep water old enough to account for elevated atmospheric ^{14}C activity during the last glaciation and the subsequent decline that began about 16.5 ka, at least according to simple mass balance calculations (Broecker, 2004; Broecker and Barker, 2007). For example, Broecker et al. (2004) and Broecker et al. (2008) found no signal of poor ventilation at 2 km – 2. 8 km water depth in with west equatorial Pacific (WEP), nor did Broecker and Clark (2010) at 4.4 km in the east equatorial Pacific (EEP). Finally, Broecker and Clark (2011) concluded that the interplay between selective dissolution and bioturbation of planktonic foraminifera (Barker et al., 2007) is too significant to extract meaningful

ventilation ages from benthic-planktic age pairs in the deep Pacific. Evidence of significantly older bottom waters than recorded by Broecker and colleagues has been found in cores from intermediate water depths off Baja California (Marchitto et al., 2007), in the Panama Basin (Stott et al., 2009), off the Arabian peninsula (Bryan et al., 2010), in the southwest Pacific (Sikes et al., 2000; Skinner et al., 2015), and in the Southern Ocean (Burke and Robinson, 2012). It has been hypothesized that the deep reservoir mixed with near surface waters in the Southern Ocean and was introduced to Antarctic Intermediate Water (AAIW), yet the signal has not been detected along present-day AAIW pathways located along the western margins of S. America (dePol-Holz et al., 2009) and Africa (Cleroux et al. 2011).

There are several metrics for ^{14}C-based ocean ventilation (e.g. Cook and Keigwin, 2015), and of these we focus here on the difference in conventional ^{14}C ages between coexisting benthic and planktonic foraminifera (BF and PF, resepectively) which represents the extent of ^{14}C aging or disequilibrium between the surface and deep ocean. Our new ^{14}C results from several cores in the Equatorial Pacific indicate that below ~3.2 km, BF-PF ^{14}C ventilation ages were 3080 ± 1125 years during the glacial interval. The contrast of those old deep waters with younger waters above ~3.2 km, when compared to the modern $\Delta^{14}C$ distribution, likely reflects an abyssal front extending from the Southern Ocean into the tropical North Pacific Ocean, although its northern extra-tropical extent remains unclear. In addition to helping explain elevated atmospheric $\Delta^{14}C$ during the glaciation, subsequent ventilation of these old deep waters likely also influenced the postglacial decline of atmospheric $\Delta^{14}C$ and the coincident rise in pCO_2 (Marchitto et al., 2007; Anderson et al. 2009; Burke and Robinson, 2012).

2.0 METHODS

This paper presents new data on cores from four locations: the northern Emperor Seamounts in the NWP; the Gulf of California; and the west and the east equatorial Pacific (Table 1). Three of the EEP cores were collected in 1978 on R/V Knorr (KNR) cruise 73 by R.P. von Herzen for heat flow studies and were dried out by the time of our sampling. KNR73 piston cores (PCs) 3, 4, and 6 straddle the Equator in a depth transect on the west flank of the East Pacific Rise, from 3.6, 3.7, and 3.8 km water depth, respectively (Figure 1). Core 3PC was studied previously (Boyle and Keigwin 1985) and heavily sampled, so for the present study we sampled the archive half. Samples of three other EEP cores were provided by the curators at Scripps Inst. of Oceanography (PLDS 7G) and Oregon State University (VNTR01-10GC and ME0005 24JC).

Samples from WEP free fall core S67 (FFC) 15, were provided by the Hawaii Institute of Geophysics (HIG).

Sampling and analytical methods are similar to those reported earlier (Keigwin 2004). At each location we relied on $\delta^{18}O$ stratigraphy and ^{14}C dating of near-surface dwelling planktonic foraminifera (PF) to identify the glacial interval. As discussed previously, we sought to identify peaks in abundance of benthic foraminifera (BF) for ^{14}C measurement, since the burrowing action of animals on the seafloor tends to reduce the amplitude of abundance maxima but it does not usually create peaks (Broecker et al., 1984). For core ME0005 24JC, our sampling of the glacial interval was guided by the chronology of Kienast et al. (2006).

Because the KNR73 cores were dry and brittle, and not easily sampled without disturbance, we scribed the split surface at 1-cm intervals, removed large sections from the liner, and cut them along the scribe lies. Although this breaks up the sample, large pieces were collected and bagged. Small samples (1-2 g) were removed from the bags for preliminary counting. Intervals of abundant BF were re-sampled at 1-cm spacing to identify the level of peak abundance, and again if necessary until enough BF were recovered for ^{14}C measurement (generally >2 mg $CaCO_3$). Foraminifera were picked from the fraction >150 μm for both stable isotope and ^{14}C analysis. Where abundance of PF was determined (PCs 3, 4, PLDS 7G, and VNTR01-10GC), samples were microsplit to about 300 individuals and counted (>150 um fraction). The other EEP cores were still moist and sliced and bagged as above at SIO and OSU, and the WEP free fall core (FFC) was sampled using paleomagnetic cubes by the curator at HIG.

BF samples were cleaned ultrasonically if necessary, and planktonic samples were cleaned this way only if they were abundant. Smaller samples were put in 1 dram screw cap vials filled completely with distilled water. The vials were shaken to suspend the foraminifera and then quickly hit against the lab bench. This “infrasound” treatment successfully shakes free loosely adhering sediment without too much damage to the shells and is easier to control than ultrasound.

Emperor Seamount results and previously published data from shallow locations in the nearby Okhotsk Sea are based on the benthic foram *Uvigerina* and the planktonic *Neogloboquadrina pachyderma* s. because these are the only species present in the glacial interval that were sufficiently abundant for ^{14}C measurement. During warm episodes of deglaciation, ^{14}C dates were on *Globigerina bulloides* and *Uvigerina*. *Uvigerina* was also analyzed from the

LGM of DSDP Site 480 samples in the Gulf of California (Keigwin and Jones, 1990). In the Equatorial Pacific we dated the PF *Globigerinoides ruber* and *Globigerinoides sacculifer*, and the BF *Nuttalides umbonifera, Uvigerina*, and *Cibicidoides*. Low BF abundance and lack of obvious abundance maxima led us to date mixed BF in ME005 24JC, but *Uvigerina* was the most abundant taxon.

Accelerator mass spectrometry (AMS) ^{14}C dating was done using routine methods at the National Ocean Sciences AMS (NOSAMS) facility at Woods Hole Oceanographic Institution and at the Univ. of California, Irvine, for samples graphitized at the Univ. of Colorado. All ^{14}C ages are given as the conventional laboratory reported age, without correction for ocean reservior effects (Stuiver and Polach, 1977). Most stable isotope measurements were made at NOSAMS on a VG Prism mass spectrometer and some were made on a Finigan 252. Where possible, we made analyses on individual specimens of *Uvigerina*, *Cibicidoides*, or *N. umbonifera*.

3.0 RESULTS

3.1 Equatorial Pacific.

New stable isotope, abundance, and ^{14}C results for Equatorial Pacific cores are summarized in Figure 2 and arranged according to water depth. Stable isotope data are archived at the National Climate Data Center (http://search.usa.gov/search?affiliate=NCDC&query=paleo). Where multiple benthic measurements were made at the same level (within 1.0 cm), we report the apparent ventilation age as determined from each benthic species as the difference between the ^{14}C age for that species and the average of the PF ^{14}C ages for that level. All new ^{14}C results and ventilation ages are listed in Table 2. Uncertainty in average PF age is given as the standard error (SE) of the mean of the measurement values or the individual measurement uncertainties summed in quadrature, whichever is larger. Uncertainty of BF-PF ventilation age estimates was calculated as the quadrature sum of the 1σ BF measurement uncertainty and the PF age uncertainty (where only a single PF age is available, the average SE for all PF measurement pairs was used). Where we have AMS dates on multiple BFs from the same stratigraphic level, we calculated ventilation ages for each BF sample separately. Thus, one core depth may provide multiple ventilation age estimates.

For purposes of the present study, we define the glacial interval as between 25 and 15 ^{14}C ka measured in PF. Data are considered to be glacial if

one of a pair of PF dates falls within 1σ of the 15-25 ^{14}C ka window. Above ~3.7 km water depth, the glacial interval (shaded interval in Figures 2-4) is found between about 40 and 80 cm, but at greater water depths it appears closer to the core top. As expected, where $\delta^{18}O$ is maximum $\delta^{13}C$ is at or near minimum, and the glacial $\delta^{13}C$ of individual *Cibicidoides* is within the range of previous studies.

The benthic fauna changes as a function of water depth, and of the three genera we counted, only *Cibicidoides* are found at all water depths. At all but the deepest site, in the WEP, and the easternmost site (24JC), *Cibicidoides* reach peak abundance during the glacial interval. Above ~3.7 km there are short maxima (a few cm) of *Cibicidoides* within or just above this interval, and these are usually associated with maxima in *Uvigerina* and sometimes with *N. umbonifera* maxima. However, there are no *Uvigerina* in the WEP at 4.25 km, and there are no *N. umbonifera* above about 3.4 km water depth in the EEP. At the two KNR 73 cores between 3.6 and 3.7 km in the EEP, *N. umbonifera* is most abundant before 25 ^{14}C ka and in the Holocene.

The abundance of *G. ruber*, *G. sacculifer*, and total planktonic foraminifera also show substantial variability (Figure 3). The two *Globigerinoides* spp. represent about 10% of the planktonic fauna, on average, and they reach a broad maximum in abundance during deglaciation. Abundances are lower during the glacial and the Holocene (~upper 20 cm), and (oddly) in the two cores with the thickest Holocene sections, the more solution-susceptible *G. ruber* (Berger, 1970) is consistently least abundant.

3.2 Northwest Pacific.

Of the many ^{14}C dated sites in the NWP, results from two examples are presented in Figure 4 (see also Cook and Keigwin, 2015). All cores from this region contain abundant *Uvigerina* during deglaciation [Keigwin, 1998], but abundance of this genus during the LGM is usually lower, and we have not found clear glacial peaks in BF abundance deeper than 3.3 km on the northern Emperor Seamounts. In both RNDB 11PC and Vinogadov 37 GGC (3225 and 3300 m, respectively, on Detroit Seamount) it was necessary to sample both the working and the archived halves of the cores in order to obtain a datable number of *Uvigerina*. Figure 4 shows only the 11 PC data, as an example. The shape of the small LGM *Uvigerina* peak at ~110 cm is identical in each half of the core, and $\delta^{18}O$ measurement of individual *Uvigerina*, the $\delta^{18}O$ on *N. pachyderma s.*, and the dates on *N. pachyderma s*. all indicate that the small LGM peak did not result from down core reworking of specimens from the much larger deglacial peaks. The three deglacial peaks yield PF ^{14}C ages that are all between 13.08 and 13.14 ^{14}C ka.

In contrast to the results at Detroit Seamount (50°N), Tenji Seamount core RNDB 13PC (49°N) has two LGM BF peaks, based on $\delta^{18}O$ and PF ^{14}C ages (Figure 4). This core also has three deglacial maxima in *Uvigerina* abundance, with 4 PF ages of between 13.00 and 13.66 ^{14}C ka. Late in deglaciation, 13PC has two additional BF abundance maxima, but the $\delta^{18}O$ data do not reach the expected Holocene minimum of <3.5 ‰. The accompanying trigger core (13PG) has only one late deglacial BF maximum and we consider that core to be more reliable than the piston core because it captures the expected Holocene $\delta^{18}O$ minimum.

4.0 DISCUSSION

Our observations of millennial scale changes in BF abundance in the EEP are evidently new. The abundance patterns in Figure 2 have not been noted previously, presumably because earlier sampling of EEP cores was done too coarsely to resolve the millennial-scale events described here. (Most of the BF peaks in the NWP and the EEP occur within a 5 cm interval of core.) Furthermore, most previous authors have not measured the dry mass of their sediment samples so it is impossible to know if there have been changes in absolute BF abundance.

Despite the generally low sedimentation rates in our cores (all <7 cm/kyr except for ME0005 24JC, >20 cm/kyr), where present, benthic foram abundance maxima are several times larger than background values (Figure 2). This suggests that they result from some process significant enough to survive the effects of bioturbation. As bioturbation has often compromised detection of possible millennial scale climate signals in the Equatorial Pacific, the strong BF abundance signal documented here may hold promise for regional (and beyond) correlation of events.

Below, we first consider possible contributions of surface ocean fertility and sediment transport to observed BF abundance maxima, followed by a discussion of the possible influences of dissolution and bioturbation on our ^{14}C results. We then present a basin-wide compilation of glacial BF-PF ventilation ages by depth that appears to indicate a widespread abyssal front in the glacial Pacific.

4.1 Significance of BF abundance changes.

4.1.a. *BF abundance maxima and export production of organic carbon*.

A long history of studies concluded there must have been higher surface ocean fertility in the EEP during glacial maxima (Arrhenius, 1952; Rea et al.,

1991; Herguera and Berger, 1991). At the eastern end of our study area, in the Panama Basin, *Uvigerina* is thought to respond to increased export production of carbon in terms of both increased size and abundance (Pedersen et al., 1988). Loubere (1991) made a statistical regression of BF species percentages and surface productivity in EEP core tops and found the fauna highly responsive to productivity. In particular he noted that *Uvigerina*, *Cibicidoides* and *Melonis barleeanum* are associated with highest organic export fluxes close to the Equator. Conversely, *N. umbonifera* was found to be typical of a lower productivity assemblage that is more prominent south of 5°S. Based on Loubere's (1991) work, our EEP results indicate highest productivity occurred generally in the late glacial/early deglacial interval, a conclusion supported by geochemical evidence for changing redox conditions (Berger et al., 1983).

In the Panama Basin, a broad deglacial maximum in the mass accumulation rate of organic carbon and cooling of the sea surface has been documented by Kienast et al. (2006), with a mid-point PF conventional ^{14}C age of ~13.9 ka. Far to the northwest on the Emperor Seamount chain, mass accumulation rates of opal, calcium carbonate, organic carbon, and benthic foraminiferal abundance, indicate higher fertility during the last deglaciation compared to the LGM and the Holocene (Keigwin et al., 1992; Keigwin 1998). High export production was confirmed by accumulation rates determined by Th normalization in nearby cores (Crusius et al. 2004; Kohfeld and Chase, 2011), and in the Gulf of Alaska by increased diatom export, Ba/Al, and $CaCO_3$ (Galbraith et al. 2007). Galbraith et al. (2007) argued that these changes occurred abruptly in the Gulf of Alaska at the onset of the Bolling/Allerod interval in the North Atlantic region (~14.5 cal. ka), with ^{14}C age constraints from loosely bracketing conventional PF ages of 13.0 and 15.1 ^{14}C ka.

Among our EEP cores, PLDS 7G, VNTR01 10GC and KNR73-3PC contain BF abundance maxima with PF ^{14}C ages of ~14.15, 14.18 and 14.73 ^{14}C ka, respectively (Fig. 2) that indicate that they may be broadly synchronous with the previously documented productivity increase in the Panama Basin (Kienast et al., 2006), after allowing for possible regional gradients of deglacial reservoir age of several hundreds of years (Lindsay et al. 2015.; Rae et al. 2014). Similarly, the multiple BF abundance peaks with PF ^{14}C ages of 13.0 to 13.6 ^{14}C ka in our NWP cores (Fig. 4) may be related to the sudden increase in productivity in the northern Pacific (Keigwin et al. 1992; Galbraith et al. 2007; Kohfeld and Chase, 2011).

In the four EEP cores in which we have counted planktonic foram abundance, highest abundances generally occur during deglaciation, but the broad deglacial rise in planktonic species does not usually contain abundant benthic taxa (Fig. 3). Although planktonic foraminifera are most abundant

during the deglacial interval, we cannot be sure to what extent this reflects preservation rather than productivity (Berger, 1992, for example), or sediment focusing (Marcantonio et al., 2001; Kienast et al., 2006).

4.1.b. *Sediment transport.* Although there is strong evidence for high productivity in the NWP during deglaciation and in the EEP during glaciation, it remains possible that peaks in BF abundance could be an artifact of extensive winnowing of clay and silt. In the case of extreme and persistent winnowing, BF peaks could be created. However, in order to explain increases in benthic abundance by factors of 5 or 10, such as during the Holocene or the events at ~14.7 and 15.5 ^{14}C ka in cores 3PC and 4PC, respectively (Figure 2), enrichment by winnowing would have necessarily produced substantially condensed intervals. Our dating of these cores was not designed to test this possibility, but the depth distribution of PF ^{14}C ages in 3PC and 4PC is inconsistent with the presence of large discontinuities. At the Emperor Seamounts, each site has multiple deglacial peaks in *Uvigerina* associated with similar PF ^{14}C ages of ~13.1 ^{14}C ka, but the maximum abundances at core 11PC are ~50/g whereas at core 13PC it is ~28/g. If these events resulted from winnowing, then one would expect more winnowing at 11PC, yet based on the *Uvigerina* δ^{18}O, the two cores have similar rates of sedimentation.

4.2. Planktonic age bias due to selective dissolution and bioturbation.

Barker et al. (2007) noted that the effects of selective dissolution of surface dwelling planktonic species such as *G. sacculifer* and *G. ruber* compared to deeper-dwelling planktonics, variable residence time of shells in the sediment surface mixed layer, and low rates of sedimentation can combine to create ^{14}C age offsets between different PF species from the same sediment sample. The conceptual model predicts that relatively dissolution prone species will show a young ^{14}C age bias with respect to dissolution resistant species, as a result of selective removal of older tests from the mixed layer population. Broecker and Clark (2011) proposed that this effect could lead to artificially large ventilation ages that are based on the difference between BF ^{14}C dates and PF ^{14}C dates from co-deposited dissolution prone surface dwelling species. For example, they noted that in four of seven deep water core tops from the equatorial Pacific that are today bathed by calcite undersaturated water, *G. sacculifer* has a ^{14}C age about 1000 years younger than solution-resistant planktonic species. Comparison of PF ages from paired measurements of *G. ruber* and *G. sacculifer* in cores 3PC and 4PC provide some insight into the importance of this process in the deep EEP as, even though both species are

surface-dwellers, *G. ruber* is known to be less resistant to dissolution than *G. sacculifer* (Berger, 1970).

We find no statistically meaningful inter-species age difference across all available *G. ruber* and *G. sacculifer* measurement pairs (n = 17, Table 3). If we break the pairs out according to time intervals (based on average PF ^{14}C ages) corresponding broadly to the Holocene (0-10 ^{14}C ka), deglaciation (10-15 ^{14}C ka), and the glacial period (15-25 ^{14}C ka), we find that only for the deglacial period is *G. ruber* measurably younger than *G. sacculifer* (-233 ± 112 ^{14}C yr, n = 6). For the glacial interval, the relationship is marked by large variation in both magnitude and sign (+59 ± 745 ^{14}C yr, n = 7). These results, along with an analysis of the absolute deviation of the inter-species differences (Table 3), suggest that the observed age differences are largely randomized by bioturbation and generally do not preserve systematic offsets that might arise from differential dissolution in the mixed layer or from ecological habitat preferences (which are expected to be similar in the EEP for these two species, for example, Watkins et al. 1996). The results are, furthermore, largely insensitive to the placement of age boundaries in the analysis.

We also note that the effect described by Barker et al. (2007) is based on modern ocean observations and late Holocene sediment that reflect especially corrosive conditions on the sea floor. However, glacial and deglacial sediment is generally thought to be better preserved than Holocene sediment in the Equatorial Pacific. All other things being equal, the impacts of selective dissolution and young PF age biases should then be greater in the Holocene than during the glaciation and deglaciation, reducing rather than enhancing observed differences in ventilation age that might otherwise arise due to relative aging of Pacific deep water during glacial times. Our Holocene observations are limited to only two cores (3, 4PC), but with BF-PF ventilation ages of 1000 to 2000 years, they are close to the expected values based on modern observations (~ 1600 yrs; Broecker et al., 1984). As we describe below, BF-PF ventilation ages in the glacial and early deglacial deep Equatorial Pacific are much higher and more variable. In our view, the largest contribution to uncertainty is from bioturbation which, for PFs, we estimate conservatively to be on the order of ± 500 yr based on absolute deviations of PF age pairs for the glacial period (Table 3). Since we have sampled BFs at local peaks of absolute abundance, uncertainties in BF ages from sediment mixing should be minimized, and are likely more than adequately captured by differences in ventilation age for different BF species sampled at or near the same stratigraphic level (Fig. 2, Fig. 5).

4.3. Equatorial and North Pacific BF-PF ventilation age.

There is general agreement that there were significant changes in the deep circulation of the North Pacific during the past ~25 ka, as evident in various proxy data (Boyle and Keigwin, 1985; Zahn et al., 2001; Keigwin, 1998; Ohkushi et al., 2003; Galbraith et al., 2007; Okazaki et al. 2010; Lund et al. 2011). Of the many proxies brought to bear on the subject, ^{14}C has been of recent interest because of the suggestion that the deep ocean may have driven the deglacial atmospheric pCO_2 increase and $\Delta^{14}C$ decrease if long-sequestered CO_2 was released to the atmosphere as deep ocean ventilation increased after the glacial period (Hughen et al., 2004; Broecker et al. 2004; Marchitto et al. 2007; Skinner et al. 2010). Okazaki et al. (2010) compiled available BF -PF ^{14}C age pairs from North Pacific locations and concluded that BF-PF ventilation ages began to decrease beginning 20-19 calendar ka and remained ~500-1000 ^{14}C yr lower than during the early LGM until the end of Heinrich Event 1 (H-1, 17.5 to 15 cal. ka), suggesting that deep water may have been produced somewhere in the region to depths as great as 3 km during the interval. More recently, Rae et al. (2014) showed that ventilation of the deep NEP (3640 m) improved suddenly during "the middle of H-1" based on a brief but seemingly robust collapse of the age difference in two BF-PF pairs. ^{14}C results from another NEP core indicate that ventilation at 2.7 km was the same during the last glaciation as today (Lund et al. 2011). On the other hand, Jaccard and Galbraith (2013) suggest that bottom waters at 2400 m (and deeper) were poorly ventilated until ~ 15 calendar ka based on measurements of authigenic uranium in NWP core 13PC. Aside from four BF-PF pairs of Shackleton et al. (1988) and the previous work of and Broecker et al. (2004, 2008) and Broecker and Clark (2010), ours are the only other deep water ventilation estimates from the Equatorial Pacific.

Whereas Okazaki et al. (2010) compiled ventilation data from the North Pacific in a time series, here we compile the data they used along with more recently published data and our new results into a single depth reconstruction, but with distinct labels for results from the NWP, NEP, EEP and WEP (Figure 5). In our analysis we consider primarily the BF-PF ventilation age, since this metric does not involve assumptions regarding reservoir age effects or calibration to calendrical age, as may be needed to estimate physical ventilation age using decay trajectories (c.f. Adkins and Boyle, 1997). Thus, plotted results are not subject to potentially significant uncertainties regarding the magnitude and spatial distribution of past surface reservoir ages, but ventilation ages with respect to the coeval atmosphere may be more variable than indicated by the reconstruction based on BF-PF age.

We also lump together all results for which any one of the associated conventional PF ^{14}C ages lies within 1σ of 15 to 25 ^{14}C ka, a relatively broad interval that includes both the LGM and H-1. The approach is deliberately inclusive so as to maximize the number of (still relatively sparse) observations under consideration and because climatically and oceanographically significant events documented elsewhere are not always well resolved in the Pacific Ocean. For example H-1 is not directly evident in the Pacific as an armada of icebergs and is otherwise difficult to identify with certainty. Furthernore, as has been noted previously (Keigwin et al., 1992; Skinner and Shackleton, 2005), Pacific BF $\delta^{18}O$ data lag Atlantic data because of the long interbasin transit time, so from that perspective the end of the LGM in the deep Pacific is younger than in the Atlantic. Glaciological evidence from Hawaii indicates the LGM persisted in the North Pacific until about 15 ka (Blard et al., 2007).

The glacial BF-PF ventilation age results are given in Figure 5 along with an estimate of the basin-wide average $\Delta^{14}C$ in modern seawater (solid red line, upper X axis scale) by depth from the World Ocean Circulation Experiment (http://cdiac.ornl.gov/oceans/glodap/), and were averaged over the North Pacific between the Equator and 55°N by R. M. Key (pers. comm.). Data used in making Figure 5 are listed as SOM Table 1. Equivalent sea water ^{14}C ages (open red symbols) are effectively relative to that of the pre-nuclear, pre-industrial atmosphere and have been corrected by 400 yrs for presentation on the BF-PF age scale (lower X axis). Formal uncertainties for the apparent ventilation ages were desribed earlier and are listed in Table 2; a more realistic assessment may be provided by the observed spread in BF-PF age differences for different cores from similar depths in the same ocean region or, (for the new results) for different BF species sampled at or near the same stratigraphic level. Since the glacial data span a relatively large age interval, some of the observed spread may reflect authentic time dependent variability of BF-PF ventilation age. As we will show below, however, plausible time-dependent variations (i.e., Okazaki et al. 2010) do not appear to have influenced the overall structure of the BF-PF depth profile.

Despite the observed scatter, the glacial age sediment data are roughly consistent with the modern sea water ^{14}C profile at depths above ~3.2 km (Figure 5). A distinctive break relative to the modern profile occurs about 3.1 km in the sediment results from the Equatorial Pacific; data between 1.9 and 3 km average 1610±250 yrs,whereas deeper data fall consistently on the “old” side of the modern profile, with an average BF-PF ventilation age of 3080±1125 yrs. Taken at face value, these results record a pronounced abyssal front between shallower, well ventilated waters and deeper, poorly ventilated waters in the Equatorial Pacific at a modern water depth of 3.0 to 3.2 km. The

impression of a front is reinforced by consistency of equatorial Pacific and North Pacific results above 3.0 km. Four BF-PF pairs from 3.2 km in the EEP (Shackleton et al. 1988) are consistent with a front at or just above this depth (SOM Fig. 2), but are excluded from Fig. 5 since, unlike the other EEP data, they are based on PF measurements in *N. dutertrei* which may be biased old (potentially reducing BF-PF with respect to other data shown) (Barker et al., 2007). Inclusion of these data would yield a deep Equatorial Pacific BF-PF average of 2890 ± 1100 yr.

In order to evaluate the possible influence of time-dependent variation in our reconstruction, we separate glacial results into two age classes, greater or less than ~19.6 ± 0.4 calendar ka, corresponding to the transition to younger BF-PF ventilation age documented above ~ 3km in the North Pacific (Okazaki et al. 2010). This age break corresponds to conventional PF ^{14}C ages greater or less than 17.0 ^{14}C ka in our results (Table 2), with an age spread after calibration that incorporates large uncertainty in the surface reservoir age (ΔR of 0-600 in CALIB 7.1, after Stuiver and Reimer 1993) but which nevertheless securely identifies samples older than the transition indicated by Okazaki et al. (2010). For the deep Equatorial Pacific, there is no statistically signficant difference of BF-PF age for pre- and post transition samples; "pre-transition" samples are 2850 ± 870 yr (n=9) and "post-transition" samples are 3440 ± 1440 yr (n=6) and 2920 ± 750 yr (n=5) when the oldest (6050 yr) sample is excluded. Most importantly, the large contrast with results above and below 3.1 km is maintained both within and across the two age classes, as can be seen in separately annotated symbols in Figure 5. We also note that some of the time-dependent variation reconstructed by Okazaki et al. (2010) may relate to changes in the range of depths represented by their core selection, since the largest BF-PF ages in the North Pacific appear to be in "pre-transition" samples from 2.4 to 2.9 km.

Any possible northern manifestation of poorly ventilated waters within the deep N. Pacific remains difficult to evaluate from our compilation of results. Above ~3.1 km, both the northern and Equatorial Pacific measurements indicate similar BF-PF ventilation ages. This is likely a robust finding, since similar methods were employed in both areas (most NWP results used our methods; Cook and Keigwin, 2015). Below ~3.1 km, there is a paucity of glacial BF-PF age pairs from the northern N. Pacific that meet our criteria for co-deposition (within 1 cm). Of these, 2 come from the relatively brief "middle H-1" ventilation event documented in the NEP by Rae et. al. (2014) and, they suggest, these were associated with a dramatic increase in the surface ocean reservoir age (leading to under-representation of the actual deep water ^{14}C age from BF-PF age pairs). We note that many of the deepest northern N. Pacific

cores come from areas where today the surface ocean reservoir age appears to be locally elevated (see map of core depths vs. estimated pre-nuclear surface water ^{14}C age in Supplementary online Figure 1. If the estimated recent, pre-nuclear reservoir age distribution (Rubin and Key, 2002) reflects the potential for locally- or regionally- anomalous increases in reservoir age during the glacial and/or deglacial periods, results from deeper N. Pacific cores in Fig. 5 may under-represent actual deep water ^{14}C ages with respect to the larger number of records available from above ~3.1 km. Nonetheless, there is as yet no clear ^{14}C evidence for excessive glacial aging of deep waters in the northern N. Pacific. The single new BF-PF age pair characterizing the deep NWP, as noted in section 3.2, ultimately required sampling of the archive half of Vinogradov 37GGC in order to obtain enough *Uvigerina* for dating. Given that this is the only result for the deep NWP, more work in the region is clearly needed.

Radiocarbon data from the LGM of the subtropical western North Atlantic indicate apparent ventilation ages of only about 1500 years in cores as deep as 4.7 km (Keigwin, 2004). Evidently the very old deep water we find in the Equatorial Pacific Ocean did not extend substantially unmixed into the deep western North Atlantic. In the South Atlantic at ~3.8 km Skinner et al. (2010) also measured LGM BF-PF ventilation ages of about 1500 years. However, they also identified large changes in the surface reservoir age, suggesting that that deep South Atlantic benthic ^{14}C ages were 3500 to 4000 yrs older than the coeveal atmosphere during the LGM. Values in this range were maintained for ~6 kyr, with a maximum at ~19 calendar ka BP. In Figure 5 we show prior estimates of $\Delta^{14}C$ (vs. coeval atmosphere) for these data as a box centered at 3.8 km depth to represent a likely end-member value for Lower Circumpolar Deep Water (LCDW) (Burke and Robinson, 2012). Projection of these results from the $\Delta^{14}C$ (vs. atmosphere) axis onto the BF-PF age axis carries some uncertainties related to possible local deviations from mean ocean surface reservoir age, but the overall impression is that both the deep Equatorial Pacific and deep Southern Ocean were comparably aged during much of the LGM. We thus posit a direct connection between the two locations via mixing with LCDW as in the present day ocean, implying that similarly old waters may have had a circumpolar distribution during part or all of the glacial period.

Thus, we argue that both the Southern Ocean (Skinner et al. 2015), and much of the world's most voluminous ocean basin harbored a potentially vast reservoir of old carbon. Broecker et al. (2004) estimated that the volume and degree of deep ocean ^{14}C depletion needed to account for the equilibrium change in $\Delta^{14}C$ of glacial atmosphere and remaining portions of the ocean was much larger than seemed plausible given existing observational constraints.

However, Burke and Robinson (2012) suggest that recent observations of abyssal depletion during the LGM, comparable in degree to those documented here, would be sufficient to account for subsequent transient depletion of the atmosphere and surface ocean during deglaciation. The complementary observations of deglacial atmospheric $\Delta^{14}C$ and CO_2 change (Machitto et al. 2007) suggest a common cause relating to improved ventilation of the ocean's deepest waters (Toggweiller et al., 2006).

CONCLUSIONS

Our study of deep ocean ventilation ages based on the difference in ^{14}C ages of coexisting benthic and planktonic foraminifera in cores from the deep Equatorial Pacific and Northwest Pacfic reveals the following:

1. Maxima in absolute abundance of benthic foraminifera are common in both the NWP and most Equatorial Pacific sites during the Holocene, the deglaciation, and the glacial period. They appear to be related to higher fertility during glaciation in the EEP and during deglaciation in both regions. Abundance of planktonic foraminifera is lowest in the late Holocene, intermediate during the glacial, and highest during deglaciation.

2. In the EEP, paired ^{14}C measurements of *G. sacculifera* and *G. ruber* do not reveal systematic differences of age that might arise from ecological preferences or differential dissolution in the sediment mixed layer. Variations in the sign and magnitude of inter-species age differences can be attributed largely to bioturbation.

3. Our few Holocene apparent ventilation ages from the EEP fall in the 1000 to 2000 year range, similar to today. However, deglacial and glacial values are both larger and more variable (1500 to 6000 years), with a mean of ~3100 yrs that is greater than anything observed previously in the shallower Equatorial and North Pacific. Data above about 2 km indicate slightly younger ventilation ages compared to the modern (GLODAP) mean sea water depth ^{14}C profile for the same region. A large contrast of apparent ventilation age (~1500 yrs) above and below 3.1 km in the Equatorial Pacific is emphasized by comparison to the modern data, suggesting a front in BF-PF ventilation age near that depth.

4. The large BF-PF 14 C differences for >3.1 km in the glacial equatorial Pacific indicate bottom waters that may be comparably aged to the Lower Circumpolar Deep Water in the South Atlantic. Thus, there may have been a

circupolar distribution of old water that extended as far as the equatorial Pacific and that was likely sufficient to have caused the transient decrease in atmospheric radiocarbon activity during deglaciation.

ACKNOWLEDGEMENTS

We thank Mary Carman for helping prepare samples for geochemical analysis, Al Gagnon for providing the stable isotope data, and the staffs at NOSAMS and UC Irvine for radiocarbon measurements. Chad Wolak and Patrick Cappa assisted with sample preparation at the Univ. of Colorado. Bob Key has been especially generous with his time in compiling North Pacific WOCE data for our reconstructions. We also thank Ning Zhao for providing ^{14}C results from EEP core 24J, and Colin Lindsay for preparing the supplementary figure. We are also grateful to the curators at HIG, OSU, and SIO for for carefully sampling cores in their collections. The manuscript was greatly improved by the thoughtful comments of Luke Skinner and an anonymous reviewer. This work was funded by NSF grants OCE-1031224 and OCE-0424861 to LDK and 0851391 to SJL.

REFERENCES

Adkins, J. F. and E. A. Boyle (1997). "Changing atmospheric $\Delta^{14}C$ and the record of deep water paleoventilation ages." Paleoceanography **12**: 337-344.

Anderson, R., S. Ali, et al. (2009). "Wind-driven upwelling in the Southern Ocean and the deglacial rise in atmospheric CO2." Science **323**: 1443-1447.

Arrhenius, G. (1952). "Sediment cores from the east Pacific." Rep. Swedish Deep Sea Exped. **5**: 1-228.

Barker, S., W. Broecker, et al. (2007). "Radiocarbon age offsets of foraminifera resulting from differential dissolution and fragmentation within the sedimentary bioturbated zone." Paleoceanography **22**: PA2205.

Barnola, J. M., D. Raynaud, et al. (1987). "Vostok ice core provides 160,000-year record of atmospheric CO2." Nature **329**: 408414.

Berger, W. (1970). "Planktonic foraminifera: selective solution and the lysocline." Marine Geol. **8**: 111-138.

Berger, W. (1992). Pacific carbonate cycles revisited: arguments for and against productivity control. Centenary of Japanese Micropaleontology. K. Ishizaki and T. Saito. Tokyo, Terra Scientific Publishing Co.**:** 15-25.

Berger, W. H., R. C. Finkel, et al. (1983). "Glacial-Holocene transition in deep sea sediments: Manganese-spike in the east equatorial Pacific." Nature **303**: 231-233.

Blard, P.-H., J. Lave, et al. (2007). "Persistence of full glacial conditions in the central Pacific until 15,000 years ago." Nature **449**: 591-595.
Boyle, E. A. (1988). "Vertical oceanic nutrient fractionation and glacial/interglacial CO2 cycles." Nature **331**: 55-56.
Boyle, E. A. and L. D. Keigwin (1985/86). "Comparison of Atlantic and Pacific paleochemical records for the last 215,000 years: changes in deep ocean circulation and chemical inventories." Earth and Planet. Sci. Lett. **76**: 135-150.
Broecker, W. and S. Barker (2007). "A 190 ‰ drop in atmosphere's D14C during the "Mystery Interval" (17.5 to 14.5 kyr)." Earth Planet. Sci. Lett. **256**: 90-99.
Broecker, W., S. Barker, et al. (2004). "Ventilation of the glacial deep Pacific Ocean." Science **306**: 1169-1172.
Broecker, W. and E. Clark (2010). "Search for a glacial-age 14C-depleted ocean reservoir." Geophys. Res. Lett. **37**.
Broecker, W. and E. Clark (2011). "Radiocarbon-age differences among coexisting planktic foraminifera shells: The Barker Effect." Paleoceanography **26**: PA2222.
Broecker, W., E. Clark, et al. (2008). "Near constancey of the Pacific Ocean surface to mid-depth ratdiocarbon-age difference over the last 20 kyr." Earth Planet. Sci. Lett. **274**: 322-326.
Broecker, W. S., A. Mix, et al. (1984). "Radiocarbon measurements on coexisting benthic andplanktic foraminfera shells: potential for reconstructing ocean ventilation times over the past 20,000 years." Nuclear Inst. and Methods in Phys. Res. section B: Beam Interactions with Materials and Atoms **5**: 332-339.
Bryan, S. P., T. M. Marchitto, et al. (2010). "The release of 14C-depleted carbon from the deep ocean during the last deglaciation: Evidence from the Arabian Sea." Earth Planet. Sci. Lett. **298**: 244-254.
Burke, A. and L. F. Robinson (2012). "The Southern Ocean's role in carbon exchange during the last deglaciation." Science **335**: 557-561.
Cleroux, C., P. deMenocal, et al. (2011). "Deglacial radiocarbon history of tropical Atlantic thermocline waters: absence of CO2 reservoir purging signal." Quat. Sci. Rev. **30**: 1875-1882.
Cook, M. and L. Keigwin (2015). "Radiocarbon profiles of the NW Pacific from the LGM and deglaciation: Evaluating ventilation metrics and the effect of uncertain surface reservoir ages." Paleoceanography **30, doi:10.1002/2014PA002649**.
Crusius, J., T. F. Pedersen, et al. (2004). "Elevated productivity in the NW Pacific during the Bolling warm period as a cause of reduced intermediate-water oxygen concentrations along the California margin." Geology **32**: 633-636.
Davies-Walczak, M., A. C. Mix, et al. (2014). "Late glacial to Holocene radiocarbon constraints on North Pacific Intermediate Water ventilation and deglacial atmsopheric CO2 sources." Earth and Planetary Science Letters **397**: 57-66.
dePol-Holz, R., L. Keigwin, et al. (2010). "No signature of abyssal carbon in intermediate waters off Chile during deglaciation." Nature Geosciences **3**: 192-195.
Duplessy, J. C., N. J. Shackleton, et al. (1988). "Deepwater source variations during the last climatic cycle and their impact on the global deepwater circulation." Paleoceanography **3**: 343-360.
Galbraith, E. D., S. L. Jaccard, et al. (2007). "Carbon dioxide release from the North Pacific abyss during the last deglaciation." Nature **449**: 890-894.

687 Herguera, J. C. and W. H. Berger (1991). "Paleoproductivity from benthic foraminifera
688 abundance: Glacial to postglacial change in the west-equatorial Pacific." Geology
689 **19**: 1173-1176.
690 Hughen, K., S. Lehman, et al. (2004). "14C Activity and global carbon cycle changes over
691 the past 50,000 years." Science **303**: 202-207.
692 Jaccard, S. and E. Galbraith (2013). "Direct ventilation of the North Pacific did not reach
693 the deep ocean during the last deglaciation." Geophys. Res. Lett. **40**:
694 doi:10.1029/2012GL054118.
695 Keigwin, L. D. (1998). "Glacial-age hydrography of the far northwest Pacific Ocean."
696 Paleoceanography **13**: 323-339.
697 Keigwin, L. D. (2004). "Radiocarbon and stable isotope constraints on last glacial
698 maximum and Younger Dryas ventilation in the western North Atlantic."
699 Paleoceanography **19**: doi: 10.1029/2004PA001029.
700 Keigwin, L. D. and G. A. Jones (1990). "Deglacial climatic oscillations in the Gulf of
701 California." Paleoceanography **5**: 1009-1023.
702 Keigwin, L. D., G. A. Jones, et al. (1992). "A 15,000 year paleoenvironmental record from
703 Meiji Seamount, far northwestern Pacific." Earth Planet. Sci. Lett. **111**: 425-440.
704 Kienast, M., S. S. Kienast, et al. (2006). "Eastern Pacific cooling and Atlantic overturning
705 circulation during the last deglaciation." Nature **443**: 846-849.
706 Kohfeld, K. E. and Z. Chase (2011). "Controls on deglacial changes in biofgenic fgluxes in
707 the North Pacific Ocean." Quat. Sci. Rev. **30**: 3350-3363.
708 Lindsay, C., S. Lehman, et al. (2015). "The surface expression of radiocarbon anomalies
709 near Baja California during deglaciation." Earth Planet. Sci. Lett. **422:67-74.**
710 Loubere, P. (1991). "Deep-sea benthic foraminiferal assemblage response to a surface
711 ocean productivity gradient: A test." Paleoceanography **6**: 193-204.
712 Lund, D. C., A. C. Mix, et al. (2011). "Increased ventilation age of the deep northeast
713 Pacific Ocean during the last deglaciation." Nature Geoscience **4**: 771-774.
714 Marcantonio, F., R. F. Anderson, et al. (2001). "Sediment focusing in the central
715 Equatorial Pacific Ocean." Paleoceanography **16**: 260-267.
716 Marchitto, T. M., S. J. Lehman, et al. (2007). "Marine radiocarbon evidence for the
717 mechanism of deglacial atmospheric CO2 rise." Science **316**: 1456-1459.
718 Ohkushi, K., T. Itaka, et al. (2003). "Last glacial-Holocene change in intermediate water
719 ventilation in the Northwestern Pacific." Quat. Sci. Rev. **22**: 1477-1484.
720 Okazaki, Y., A. Timmermann, et al. (2010). "Deepwater formation in the North Pacific
721 during the last glacial termination." Science **329**: 200-204.
722 Pedersen, T. F., M. Pickering, et al. (1988). "The response of benthic foraminifera to
723 productivity cycles in the eastern Equatoral Pacific: Faunal and geochemical
724 constraints on glacial bottom water oxygen levels." Paleoceanography **3**: 157-
725 168.
726 Petit, J. R., J. Jouzel, et al. (1999). "Climate and atmospheric history of the past 420,000
727 years from the Vostok ice core, Antarctica." Nature **399**: 429-436.
728 Rae, J. W. B., M. Sarnthein, et al. (2014). "Deep water formation in the North Pacific and
729 deglacial CO2rise." Paleoceanography **29**(6): 645-667.
730 Rea, D. K., N. G. Pisias, et al. (1991). "Late Pleistocene paleoclimatology of the central
731 Equatorial Pacific: Flux patterns of biogenic sediments." Paleoceanography **6**:
732 227-244.

733 Robinson, L. F., J. F. Adkins, et al. (2005). "Radiocarbon variability in the western North
734 Atlantic during the last deglaciation." Science **310**: 1469-1473.
735 Rubin, S. and R. Key (2002). "Separating natural and bomb-produced radiocarbon in the
736 ocean: The potential alkalinity method." Global Biogeochemical Cycles **16**: 1105,
737 doi:1110.1029/2001GB001432.
738 Shackleton, N. J., J. C. Duplessy, et al. (1988). "Radiocarbon age of last glacial Pacific deep
739 water." Nature **335**: 708-711.
740 Sigman, D. M., M. P. Hain, et al. (2010). "The polar ocean and glacial cycles in
741 atmospheric CO(2) concentration." Nature **466**(7302): 47-55.
742 Sikes, E. L., C. R. Samson, et al. (2000). "Old radiocarbon ages in the southwest Pacific
743 Ocean during last glacial period and deglaciation." Nature **405**.
744 Skinner, L., I. N. McCave, et al. (2015). "Reduced ventilation and enhanced magnitude of
745 the deep Pacific caron pool during the last glacial period." Earth Planet. Sci. Lett.
746 **411**: 45-52.
747 Skinner, L. C., S. Fallon, et al. (2010). "Ventilation of the deep Southern Ocean and
748 deglacial CO2 rise." Science **328**(5982): 1147-1151.
749 Skinner, L. C. and N. J. Shackleton (2005). "An Atlantic lead over Pacific deep-water
750 change across Termination 1: implications for the application of the marine
751 isotope stage stratigraphy." Quat. Sci. Rev. **24**: 571-580.
752 Stott, L., J. Southon, et al. (2009). "Radiocarbon age anomaly at intermediate water
753 depth in the Pacific Ocean during the last deglaciation." Paleoceanography **24**:
754 PA2223.
755 Stuiver, M. and H. Polach (1977). "Reporting of 14C data." Radiocarbon: 355-363.
756 Stuiver, M. and P. J. Reimer (1993). "Extended ^{14}C database and revised CALIB
757 radiocarbon calibration program." Radiocarbon **35**: 215-230.
758 Toggweiler, J. R., J. L. Russell, et al. (2006). "Midlatitude westerlies, atmospheric CO2,
759 and climate change during the ice ages." Paleoceanography **21**(2).
760 Watkins, J. M., A. C. Mix, et al. (1996). "Living planktic foraminifera: tracers of circulation
761 and productivity regimes in the central equatorial Pacific." Deep-Sea Res. **43**:
762 1257-1282.
763 Zahn, R., T. F. Pedersen, et al. (1991). "Water mass conversion in the glacial Subarctic
764 Pacific (54N, 148W): Physical constraints and the benthic-planktonic stable
765 isotope record." Paleoceanography **6**: 543-560.
766
767
768

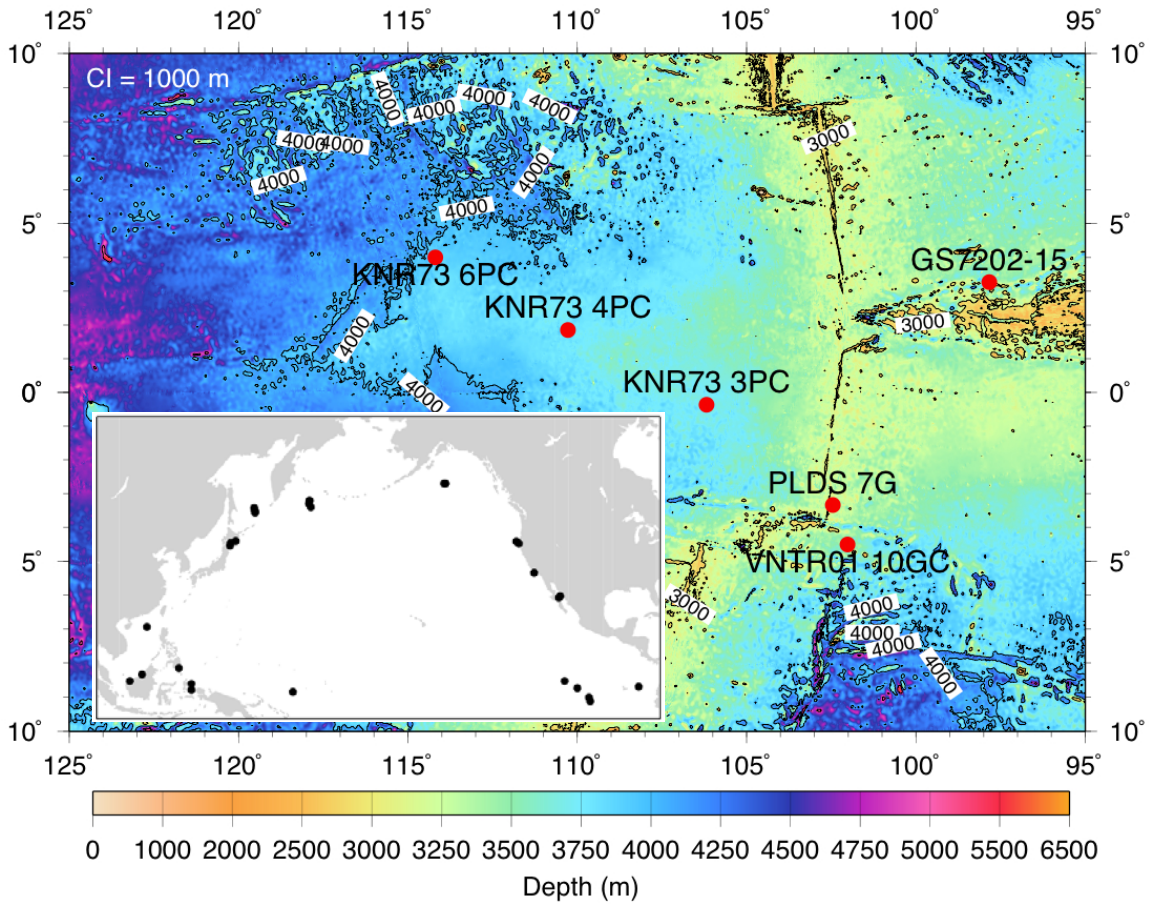
CI = 1000 m
KNR73 6PC
KNR73 4PC
KNR73 3PC
GS7202-15
PLDS 7G
VNTR01 10GC
125°
120°
115°
110°
105°
100°
95°
10°
5°
0°
0
1000
2000
2500
3000
3250
3500
3750
4000
4250
4500
4750
5000
5500
6500
Depth (m)

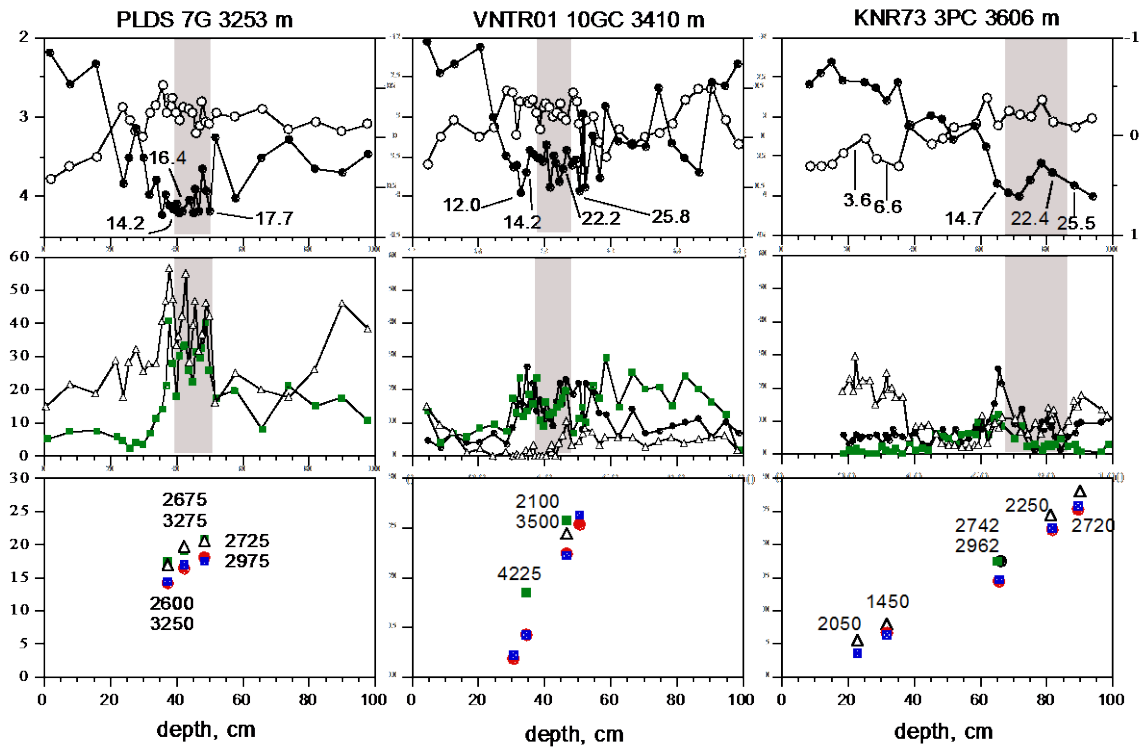

789
790

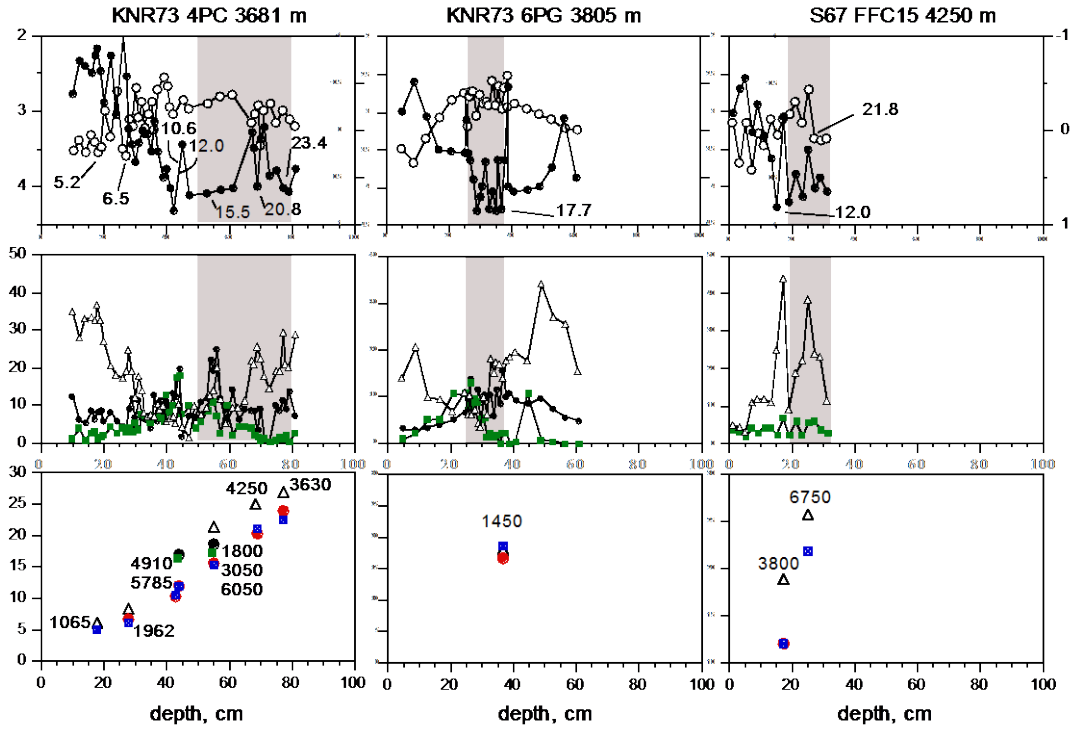

791
792

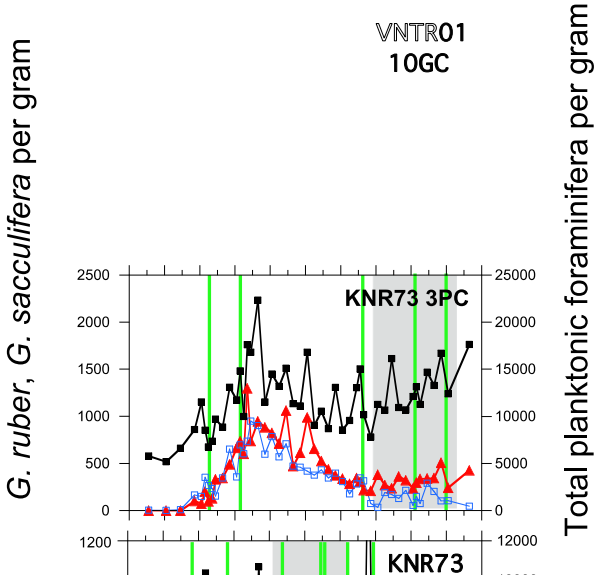
VNTR01
10GC
KNR73 3PC
KNR73
G. ruber, G. sacculifera per gram
Total planktonic foraminifera per gram
Depth, cm
2500
2000
1500
1000
500
0
25000
20000
15000
10000
5000
0
1200
12000

793

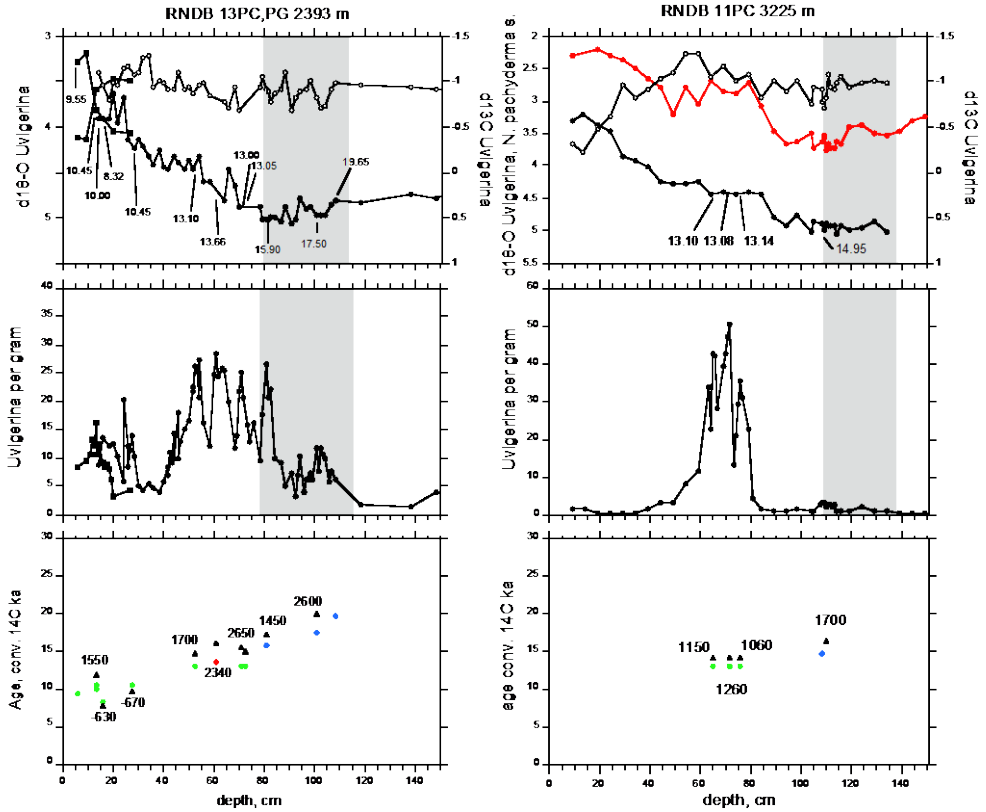
RNDB 13PC,PG 2393 m
RNDB 11PC 3225 m
d18-O Uvigerina
d13C Uvigerina
d18-O Uvigerina, N. pachyderma s
Uvigerina per gram
Age, conv. 14C ka
age conv. 14C ka
depth, cm
9.55
10.45
8.32
10.00
10.45
13.10
13.66
13.00
13.05
15.90
17.50
19.65
13.10
13.08
13.14
14.95
1550
630
670
1700
2340
2650
1450
2600
1150
1060
1260
1700

794
795

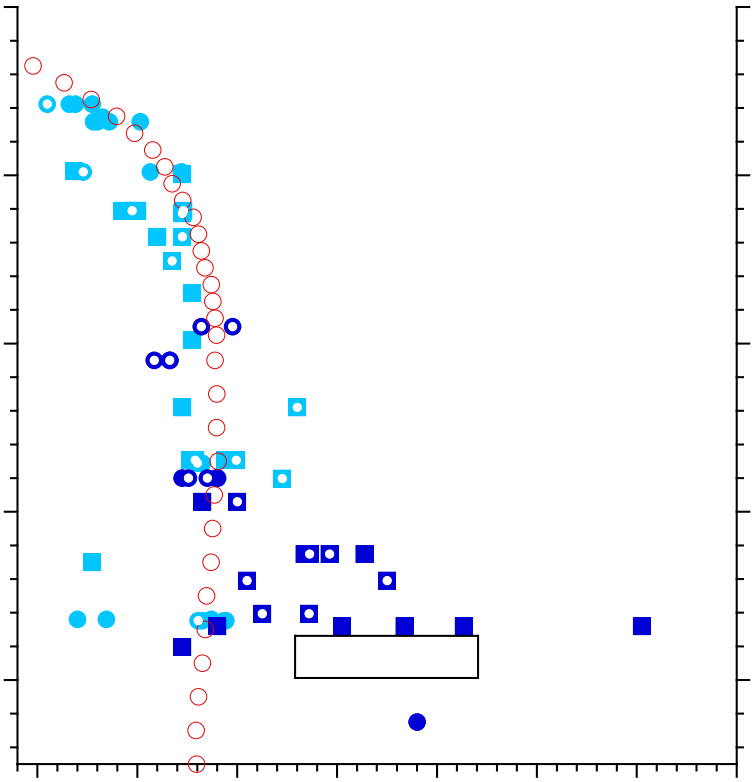

796
797